



## Bentonite and carbon nanotube adsorbents for the removal of bisphenol A from water

Noura Fathy Abdel Salam<sup>a,\*</sup>, Gabriela Kamińska<sup>b</sup>, Anna Marszałek<sup>b</sup>

<sup>a</sup>Chemical Engineering Department, Faculty of Engineering, Cairo University, Giza, Egypt, Tel.: +201099016731; email: nourafathy@eng.cu.edu.eg

<sup>b</sup>Department of Water and Wastewater Engineering, Silesian University of Technology, Konarskiego 18, 44–100 Gliwice, Poland

Received 13 March 2022; Accepted 18 September 2022

---

### ABSTRACT

The present study investigates the adsorption of bisphenol A (BPA), a well-known endocrine disruptor and widespread pollutant in the aquatic environment, using bentonite clay (Ben) and bentonite-carbon nanotubes composite (Ben-CNT) as adsorbents. In the study of adsorption isotherms, the initial concentrations of BPA in water were 1 and 2 mg/L, while for the kinetic study it was 1 mg/L. The kinetics data correlated well to a pseudo-second-order reaction, with Ben and Ben-CNT reaching equilibrium in around 60 and 180 min, respectively. Isothermal data fitted well to Freundlich and Dubinin–Radushkevich models, while the Langmuir model did not provide suitable fitting. The resulting adsorption capacity was about 1.56 and 29.61 mg/g for bentonite and bentonite-carbon nanotubes composite, respectively. The removal percentage of BPA was improved from about 24% for bentonite clay to 87% for bentonite-carbon nanotubes composite for adsorbents dose of 0.25 g/100 mL. This improvement was due to the large specific surface area of carbon nanotubes and the availability of large number of active groups for binding pollutants.

*Keywords:* Bentonite; Water; Bisphenol A; Carbon nanotubes; Adsorption

---

### 1. Introduction

There is no doubt that continuous urbanization and industrialization have disrupted the natural equilibrium of the ecology. As a result, access to safe and clean drinking water has become significantly more difficult, particularly in third-world countries. According to estimates, water-borne illnesses kill around 200 million people each year [1,2]. For example, xenobiotics such as pesticides, drugs, endocrine disruptors, personal care products, polycyclic aromatic hydrocarbons and other chemicals are entering natural water resources daily [3–5]. Bisphenol A (BPA) is an example of an endocrine disruptor that has been widely produced as a result of a variety of industrial processes, including petroleum refining, plastic production, phenolic resin

production, pharmaceutical manufacturing, coal conversion, wood preservation, metal coating, and textile dyeing [6,7].

Phenolic compounds are classified as noxious pollutants due to their highly toxic and carcinogenic nature [8,9]. Therefore, their presence in water systems is extremely dangerous to public health and the environment [10,11]. The U.S. Environmental Protection Agency has determined that the content of phenol in potable and mineral waters is 0.5 ppb, but the content of phenol in wastewater discharges is between 0.5 and 1.0 ppm [12]. BPA has been identified as a possibly priority or priority hazard substance in the Water Framework Directive [13].

As a result, developing advanced treatment techniques and materials for the effective elimination of BPA from water is critical. Several techniques such as adsorption, membrane filtration, and advanced oxidation processes

---

\* Corresponding author.

have already been developed and implemented to reduce organic pollutants such as bisphenol A [1].

Due to its simplicity, great efficiency, cost-effectiveness, and lesser secondary pollution to the environment, adsorption has been regarded as one of the most appealing treatment options for phenol removal from contaminated water [14–17]. In the adsorption process, the adsorbent type and its properties play an important role. Adsorbents such as activated carbon, carbon nanotubes and graphene oxide are considered as the most effective adsorbents for the removal of phenolic compounds from water due to their large specific surface area and functional groups [18–24]. On the other hand, a special effort has been made to use unconventional adsorbents such as waste material or natural clays [25]. Such adsorbents are cheaper and more environmentally friendly, however their adsorption capacity for phenolic compounds is lower. Therefore, different thermal or chemical modifications have already been employed to improve the specific surface area of these adsorbents [26]. Another solution is to fabricate a composite adsorbent combining properties of two different adsorptive materials such as a polymer with nanoparticles [27]. A novelty of this study is to use a bentonite-carbon nanotubes composite (Ben-CNT) for the removal of BPA from water.

Ben-CNT composite was prepared using a quick and easy method which avoided the use of harsh chemicals or high temperature. The adsorbent dose also was studied during the adsorption process, as well as the adsorption kinetics and isotherms.

## 2. Materials and methods

### 2.1. Materials

All the chemical materials used in this study were purchased as analytical grade reagents. Egyptian bentonite (Ben) powder was obtained from the Northwestern Egyptian coast and was supplied by the Egypt Bentonite & Derivatives Company (Alexandria, Egypt). The chemical composition of Ben was measured by X-ray fluorescence using an AXIOS PANalytical 2005 Instrument, where the following compositions were obtained: (in percentage by weight) SiO<sub>2</sub> – 51.33 wt.%, Al<sub>2</sub>O<sub>3</sub> – 17.64 wt.%, CaO – 6.19 wt.%, Fe<sub>2</sub>O<sub>3</sub> – 4.19 wt.%, Na<sub>2</sub>O – 2.96 wt.%, MgO – 2.67 wt.%, LOI – 11 wt.%, and traces of TiO<sub>2</sub>, K<sub>2</sub>O and P<sub>2</sub>O<sub>5</sub>. Unmodified single-walled carbon nanotubes (SWCNTs) with length 5–30 nm and outer diameter <2 nm (purity 99%) were obtained from Chengdu Organic Chemistry Co., Ltd., (Chengdu, China). Deionized water was taken directly from

Ultrapure Lab Water Systems (Rephile Bioscience Shanghai, China). Acetonitrile (ACN), methanol (MeOH) and nitric acid (HNO<sub>3</sub>) were purchased from Avantor Performance Materials (Gliwice, Poland). BPA was purchased from Sigma-Aldrich (Poznań, Poland), where its physiochemical characteristics are compiled in Table 1.

### 2.2. Preparation of bentonite-carbon nanotubes composite

The Ben-CNT composite was prepared from Ben and SWCNTs (with a weight ratio of 60:40) by previously developed methods for the preparation of clay-carbon nanotubes composite adsorbents [25]. In the first step, 18 g of Ben (particle size ~0.1 mm) was mixed with 12 g of SWCNTs. Then, 10 mL of 1% nitric acid solution containing Brij surfactant (4 g/L) was added to the powder mixture of Ben and SWCNT and mixed with magnetic stirrer at 150 rpm for 30 min. Next, the grease was heated for 120 min at 250°C in an oven. After cooling, the solid was crushed into a powder and sieved with a pneumatic sieve (Multiserw, Lubliniec, Poland) to obtain a grain size of 0.3 mm.

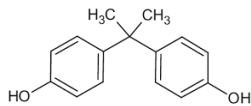
### 2.3. Characterization of adsorbents

The surface morphology of Ben and Ben-CNT composite were analyzed by scanning electron microscopy (SEM) using a JSM 6360LA instrument (JEOL, Japan). The structural properties of the adsorbents were determined by measuring the surface area and pore size distribution using the low temperature nitrogen adsorption and desorption technique according to the Brunauer–Emmett–Teller (BET) method. Nitrogen adsorption–desorption measurements were conducted at 77 K by means of a volumetric adsorption analyzer, ASAP 2010 (Micrometrics, USA).

### 2.4. Adsorption experiments

In this study, three types of adsorption experiments were performed to evaluate: (1) the removal percentage of BPA, (2) the adsorption kinetics of BPA, and (3) the adsorption isotherms of BPA. All adsorption experiments were performed using an incubator shaker at 200 rpm and 20°C. The pH of the feed water was equal to 6.5. After shaking, the adsorbent samples were separated from the liquid by filtration. To ensure quality assurance, each experiment was repeated in duplicate, and the results presented in this paper are the mean and standard deviation (error bars) of each experiment. More detailed descriptions of conducted experiments is presented below.

Table 1  
Properties of micropollutant

Compound	Chemical structure	Molecular mass <sup>a</sup> (g/mol)	logK <sub>ow</sub> <sup>a</sup> (-)	Solubility in water 20°C <sup>a</sup> (mg/L)
Bisphenol A		228.29	3.4	300

<sup>a</sup>Data obtained from: <https://pubchem.ncbi.nlm.nih.gov>

#### 2.4.1. Testing the effect of adsorbent type and dosage on removal percentage of BPA

The effect of adsorbent type and dosage on the removal percentage of BPA was studied by shaking a feed solution containing 1 mg/L of BPA with various adsorbent dosages (0.1–0.25 g/100 mL with step 0.05) in batch experiments. The removal percentage ( $R$ ) of adsorbate was calculated using Eq. (1):

$$R = \frac{C_0 - C_f}{C_0} \times 100 \quad (1)$$

where  $C_0$  and  $C_f$  are the initial and final concentrations of BPA in mg/L, respectively.

#### 2.4.2. Testing a kinetics of adsorption of BPA

Next, kinetic experiments were carried out for the Ben and Ben-CNT composite. Specifically, 0.1 g of adsorbent was added to a 250 mL Erlenmeyer flask containing 100 mL of feed water with 1 mg/L of bisphenol A. The adsorbent samples were separated from the liquid by filtration at 5, 10, 15, 30, 45, 60, 120, 180, and 240 min time intervals. The equilibrium amount adsorbed,  $Q_e$  (mg/g), was calculated from Eq. (2).

$$Q_e = \frac{(C_0 - C_e) \times V}{m} \quad (2)$$

where  $C_0$  and  $C_e$  are the initial and equilibrium concentrations of BPA in mg/L, respectively,  $m$  is the mass of adsorbent in grams (g), and  $V$  is the volume of the feed water in liters (L). The experimental data was analyzed using the pseudo-second-order kinetic model, as given in Eq. (3).

$$\frac{t}{Q_t} = \frac{1}{K_2(Q_e)^2} + \frac{t}{Q_e} \quad (3)$$

where  $Q_t$  is the amount of BPA adsorbed in mg/g at equilibrium at time  $t$ , and  $K_2$  is the pseudo-second-order constant (with units g/(mg·min)). Furthermore, based on the pseudo-second-order model, the half adsorption time,  $t_{1/2}$  (min), and the initial adsorption rate,  $h$  (mg/(g·min)), were calculated using Eqs. (4) and (5), respectively.

$$t_{1/2} = \frac{1}{K_2 Q_e} \quad (4)$$

$$h = K_2 Q_e^2 \quad (5)$$

#### 2.4.3. Testing the adsorption isotherms

Isotherm adsorption experiments were conducted with an initial BPA concentration of 1–2 mg/L (as two different concentrations), where the concentration of the adsorbents varied from 0.05 to 0.25 g/100 mL. The experimental data was fitted by three adsorption isotherm models which were the Langmuir model, the Freundlich model, and the Dubinin–Radushkevich model. Each model is briefly described in Table 2 [19,20].

#### 2.5. Water quality analysis

The concentration of BPA was measured by gas chromatograph (GC) using a 6500GC System GC-FID, YI Instrument Co., Ltd., (Hogye-dong, Anyang, Korea). The instrument was equipped with a 30 m × 0.25 mm inner diameter SLB® 5-ms fused silica capillary column of 0.25 μm film thickness (Sigma-Aldrich). Helium 5.0 was used as the carrier gas. Chromatographic analysis of BPA was performed using a temperature program for the column oven ranging from 80°C to 320°C. The injector temperature was set at 240°C. Before analysis, the compound was extracted from the samples via solid phase extraction (SPE) (phase C18, Supelco), according to a previously developed method [28].

Table 2  
Different adsorption isotherms

Isotherm model	Langmuir	Freundlich	Dubinin–Radushkevich
Assumptions	Assumes monolayer adsorption, where molecules interact only with the surface of the sorbent	Describes adsorption on heterogeneous surface energy systems. The model has significant importance for chemisorption and some cases of physisorption	Applies to adsorption systems involving only Van der Waals forces and is especially useful for describing adsorption on a microporous adsorbent
Equation	$\frac{1}{Q_e} = \frac{1}{Q_m K_L C_e} + \frac{1}{Q_m}$	$\log Q_e = \log K_f + \frac{1}{n} \log C_e$	$\ln Q_e = \ln a_{DR} - E^{-2} \cdot \epsilon^2$
Equation parameters	$Q_m$ (mg/g) is the maximum adsorption capacity and $K_L$ (L/mg) is the Langmuir fitting parameter.	$K_f$ ((mg/g)(L/mg) <sup>n</sup> ) is the Freundlich adsorption coefficient and $n$ is the number describing surface heterogeneity and sorption intensity	$a_{DR}$ (mg/g) is the amount of adsorbate that can be adsorbed in micropores (this can be obtained by plotting $\ln Q_e$ as a function of $\epsilon^2$ ), $E$ (kJ/mol) is the adsorption energy and $\epsilon$ is the adsorption potential

### 3. Results

#### 3.1. Material structure

The SEM morphology of Ben and Ben-CNT is presented in Fig. 1. Raw bentonite contains rock-like macromolecules with rough and heterogeneous surfaces (Fig. 1a). The structure of Ben is more compact compared to Ben-CNT. Additionally, in Ben-CNT, the carbon nanotubes are clearly visible on the surface (Fig. 1b). Due to the small diameter of SWCNT (2 nm) and the relatively high porosity of Ben, the SWCNT can also be located within the Ben structure.

Our previous study with Ben and Ben-CNT showed that specific surface area increased from 30.3 to 80.9 m<sup>2</sup>/g after adding SWCNT to Ben while the total volume of pores increased from 0.06916 to 0.18394 cm<sup>3</sup>/g. Additionally, the pore size was decreased from 2.1438 to 1.3781 nm [25]. The decrease in pore size of Ben-CNT compared to Ben was attributed to microporous structure of SWCNT. In other words, 40 wt.% load of SWCNT increased microporosity of Ben-SWCNT. From the results obtained in these measurements, it is clear that Ben-CNT has better sorption properties than Ben. In other words, it was worthwhile to use 40 wt.% of SWCNT to improve the properties of composite. The adsorption potential of clay adsorbents is usually limited due to the low specific surface area. On the other hand,

carbon nanotubes are expensive materials but have superior functional properties which results in the high adsorption efficiency. Thus, combining bentonite with carbon nanotubes in composite material resulted in novel and attractive adsorbent with optimum qualifications regarding to economic feasibility and removal efficiency.

#### 3.2. Effect of adsorbent type and its dose on removal percentage of BPA

As seen in Fig. 2, the adsorption of BPA was much higher on Ben-CNT compared to the adsorption found on pure Ben. It is also clear that the amount of BPA removed increases with increasing adsorbent dose. This is because a higher dose provides a higher specific surface area, and therefore more active adsorption sites [21]. More specifically, the adsorption of BPA increased from 10% to 24% on Ben and from 70% to 87% on Ben-CNT with an increasing dose from 0.1 to 0.25 g/100 mL.

#### 3.3. Adsorption isotherms of BPA on Ben and Ben-CNT

In this study, the equilibrium data obtained for the adsorption of BPA by Ben and Ben-CNT was analyzed by Langmuir, Freundlich, and Dubinin–Radushkevich

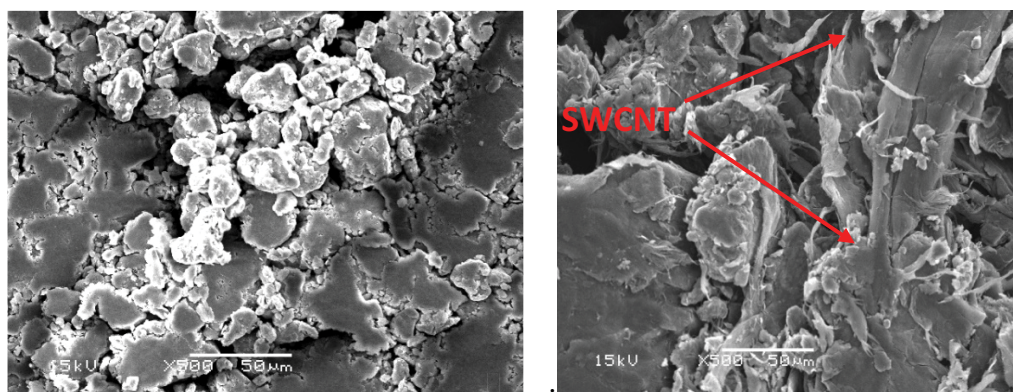


Fig. 1. SEM images of (a) Ben and (b) Ben-CNT. SWCNTs are visible in (b) as pointed out by red arrows.

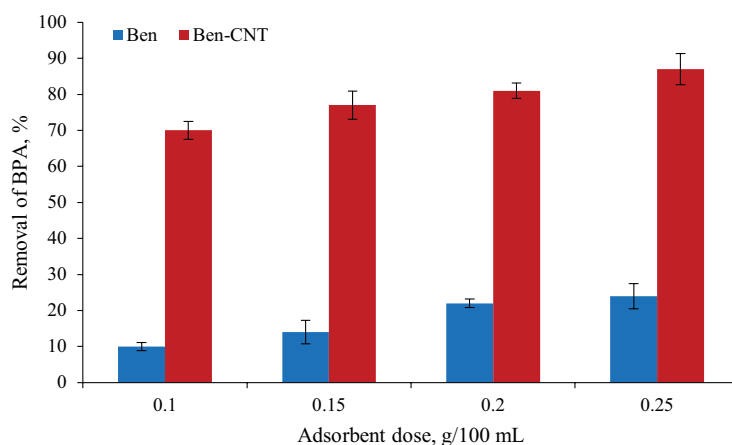


Fig. 2. Effect of adsorbent type and its dose on removal percentage of BPA ( $C_0 = 1$  mg/L).

equations. In Fig. 3, only Freundlich and Dubinin–Radushkevich isotherms are presented since they described the isothermal data well, while the Langmuir model did not provide good fitting. In other studies, the interaction between BPA and adsorbents was well described by different models and was mainly attributed to adsorbent type and its properties [29]. For example, the Freundlich and Temkin models best fitted the isotherm data for the work of Sudhakar et al. [21], with the Freundlich model also being used by the study of Cai et al. [10] to describe the adsorption isotherm of BPA on hydroxypropyl-β-cyclodextrin polymer. In contrast, the Langmuir model closely matched the adsorption isotherm data using porphyrinic porous organic polymer

as an adsorbent by the study of Lee et al. [30], and was also used by Soni and Padmaja [16] on their isotherm data.

The parameters calculated from the Freundlich, Langmuir, and Dubinin–Radushkevich models are presented in Table 3. From the values of  $K_F$  (Freundlich constant) and  $a_{DR}$  (adsorption capacity), it was identified that Ben-CNT exhibited better potential than Ben to remove BPA which, again, can be linked to the higher specific surface area of Ben-CNT composite along with its greater pore volume and smaller pore size. If parameter  $n$  from Freundlich model has a value lower than 10, this indicates that adsorption occurs on heterogeneous surface. This is in good correspondence with SEM images which show a high

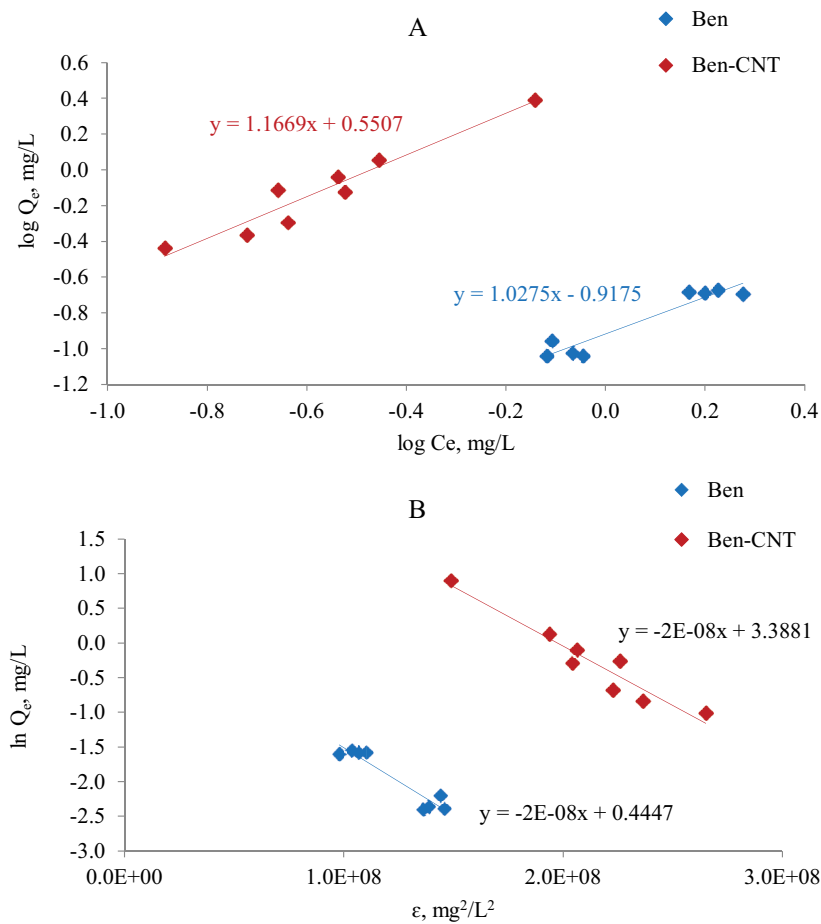


Fig. 3. Adsorption isotherms on Ben and Ben-CNT using (a) Freundlich and (b) Dubinin–Radushkevich ( $C_0 = 1–2$  mg/L, adsorbent dose: 0.05 to 0.25 g/100 mL).

Table 3

Parameters of Freundlich, Langmuir, and Dubinin–Radushkevich equations, and the correlation coefficients for the adsorption of BPA on the studied sorbents

Adsorbent	Adsorbate	Langmuir			Freundlich			Dubinin–Radushkevich		
		$Q_m$ (mg/g)	$K_L$ (L/mg)	$R^2$ (-)	$K_F$ ((mg/g)(L/mg) <sup>n</sup> )	$n$ (-)	$R^2$ (-)	$a_{DR}$ (mg/g)	$E$ (J/mol)	$R^2$ (-)
Ben	BPA	-6.447	-0.018	0.881	0.121	0.973	0.906	1.56	7,071.068	0.907
Ben-CNT	BPA	9.542	-0.268	0.883	3.554	0.857	0.927	29.61	7,071.068	0.920

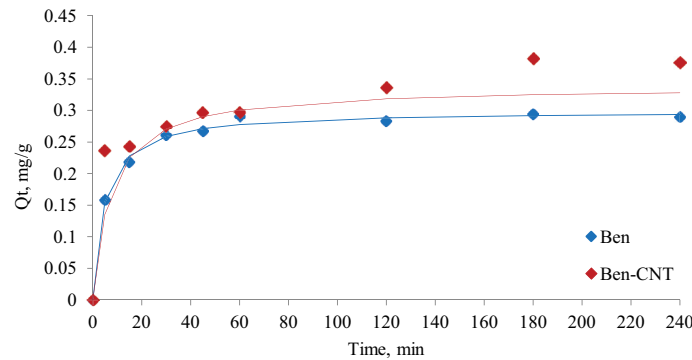


Fig. 4. Adsorption kinetic curves of micropollutants on Ben and Ben-CNT ( $C_0 = 1 \text{ mg/L}$ ).

Table 4  
Parameters for the pseudo-second-order kinetic model for the adsorption of BPA on Ben and Ben-CNT

Sample	Pseudo-second-order equation parameters						
	Adsorbate	$K_2 \text{ (g/(mg}\cdot\text{min))}$	$Q_{t(\text{exp})} \text{ (mg/g)}$	$Q_{t(\text{cal})} \text{ (mg/g)}$	$t_{1/2} \text{ (min)}$	$h \text{ (mg/(g}\cdot\text{min))}$	$R^2$
Ben	BPA	0.713	0.294	0.299	0.213	0.06	0.995
Ben-CNT	BPA	0.393	0.382	0.338	0.133	0.05	0.907

heterogeneity of surface on both adsorbents. An adsorption energy ( $E$ ) value below 8,000 J/mol suggests the physisorption of BPA on Ben and Ben-CNT [31].

### 3.4. Adsorption kinetics

The adsorption kinetic curves of BPA on Ben and Ben-CNT are presented in Fig. 4, with the calculated parameters presented in Table 4. The pseudo-second-order model describes the adsorption of BPA on both adsorbents very well. An equilibrium was reached in around 60 min for Ben and in around 180 min for Ben-CNT, which is considered quite a short time. The calculated  $Q_{t(\text{cal})}$  values corresponded well with experimental data  $Q_{t(\text{exp})}$ . This suggests that the adsorption of BPA followed second-order kinetics, and that the applied model could be used to determine the corresponding kinetic parameters. Similarly, in other studies with different adsorbents, the adsorption of BPA correlated well to pseudo-second-order kinetic equation [13–15].

Faster adsorption of BPA on Ben compared to Ben-CNT was also confirmed by the higher values of  $K_2$  (pseudo-second-order constant) and  $h$  (initial adsorption rate). Ben has a more mesoporous structure, and thus better access to its adsorption sites could be a reason for faster adsorption kinetics of BPA than on Ben-CNT. In case of Ben-CNT, the number of adsorption sites was higher. However, due to a higher microporosity, the BPA molecules needed more time to reach them. Comparing the results obtained with previous studies, it was found that the equilibrium of adsorption of BPA was reached at different times, depending on adsorbent type; for example, the adsorption of BPA onto Palm shell-based activated carbon was rapid in the first 30 min, but did not reach equilibrium until 8 h [16]. In contrast, Lee et al. [30] used fast adsorption kinetics to reach an equilibrium in 150 min. Sudhakar et al. [21] achieved equilibrium in 180 min using rice husk ash, and in 120 min using

granular-activated carbon under their optimum conditions for the removal of BPA in a comparative study.

### 4. Conclusions

In this study, the adsorption potential of bentonite clay (Ben) and a bentonite-carbon nanotube (Ben-CNT) composite for removal of bisphenol A (BPA) from water was evaluated. Adding CNTs to Ben resulted in a higher surface area and lower pore size (below 2 nm – micropores) comparing to Ben, resulting in an improved adsorption efficiency compared with using raw Ben.

The removal percentage of BPA was improved from about 24% for Ben to 87% for Ben-CNT for an adsorbent dose of 0.25 g/100 mL. Freundlich and Dubinin–Radushkevich isotherms described experimental data well for the adsorption of BPA on Ben and Ben-CNT, while the Langmuir model was not suitable for that purpose. The maximum adsorption capacity derived from the Dubinin–Radushkevich model was much higher for Ben-CNT (29.61 mg/g) than for Ben (1.56 mg/g). Similarly, the value of the Freundlich constant ( $K_f$ ) was equal to 3.554 and 0.121 for Ben and Ben-CNT, respectively. The values of adsorption energy ( $E$ ) suggested physisorption of BPA on both Ben and Ben-CNT.

The effect of adsorption dose of both adsorbents on BPA removal was also studied. It was found that as the dose of the adsorbent increased, the amount of BPA adsorbed also increased, which can be attributed to the availability of more adsorption sites. The kinetic data could also be correlated well to pseudo-second-order for both Ben and Ben-CNT adsorbents.

The adsorption of BPA reached equilibrium in about 60 min for Ben and in 180 min for Ben-CNT, where the faster adsorption of BPA on Ben was attributed to a higher mesoposity of which provided better access to adsorption sites.



## References

- [1] F.S.A. Khan, N.M. Mubarak, M. Khalid, Y.H. Tan, E.C. Abdullah, M.E. Rahman, R.R. Karri, A comprehensive review on micropollutants removal using carbon nanotubes-based adsorbents and membranes, *J. Environ. Chem. Eng.*, 9 (2021) 106647, doi: 10.1016/j.jece.2021.106647.
- [2] J. Ahmad, S. Naeem, M. Ahmad, A.R.A. Usman, M.I. Al-Wabel, A critical review on organic micropollutants contamination in wastewater and removal through carbon nanotubes, *J. Environ. Manage.*, 246 (2019) 214–228.
- [3] M. Gavrilescu, K. Demnerová, J. Aamand, S. Agathos, F. Fava, Emerging pollutants in the environment: present and future challenges in biomonitoring, ecological risks and bioremediation, *New Biotechnol.*, 32 (2015) 147–156.
- [4] K.E. Murray, S.M. Thomas, A.A. Bodour, Prioritizing research for trace pollutants and emerging contaminants in the freshwater environment, *Environ. Pollut.*, 158 (2010) 3462–3471.
- [5] P. Amoatey, M.S. Baawain, Effects of pollution on freshwater aquatic organisms, *Water Environ. Res.*, 91 (2019) 1272–1287.
- [6] O.A. Bin-Dahman, T.A. Saleh, Synthesis of carbon nanotubes grafted with PEG and its efficiency for the removal of phenol from industrial wastewater, *Environ. Nanotechnol. Monit. Manage.*, 13 (2020) 100286, doi: 10.1016/J.ENMM.2020.100286.
- [7] T.A. Saleh, S.O. Adio, M. Asif, H. Dafalla, Statistical analysis of phenols adsorption on diethylenetriamine-modified activated carbon, *J. Cleaner Prod.*, 182 (2018) 960–968.
- [8] Y.Q. Huang, C.K.C. Wong, J.S. Zheng, H. Bouwman, R. Barra, B. Wahlström, L. Neretin, M.H. Wong, bisphenol A (BPA) in China: a review of sources, environmental levels, and potential human health impacts, *Environ. Int.*, 42 (2012) 91–99.
- [9] Y. Yang, J. Yu, J. Yin, B. Shao, J. Zhang, Molecularly imprinted solid-phase extraction for selective extraction of bisphenol analogues in beverages and canned food, *J. Agric. Food Chem.*, 62 (2014) 11130–11137.
- [10] J. Cai, P. Zhang, S. Kang, W. Xu, K. Tang, Fast and efficient adsorption of bisphenols pollutants from water by using hydroxypropyl- $\beta$ -cyclodextrin polymer, *React. Funct. Polym.*, 154 (2020) 104678, doi: 10.1016/j.reactfunctpolym.2020.104678.
- [11] A. Tursi, E. Chatzisyemon, F. Chidichimo, A. Beneduci, G. Chidichimo, Removal of endocrine disrupting chemicals from water: adsorption of bisphenol A by biobased hydrophobic functionalized cellulose, *Int. J. Environ. Res. Public Health*, 15 (2018) 2419, doi: 10.3390/ijerph15112419.
- [12] E.S.Z. El Ashtoukhy, Y.A. El-Taweel, O. Abdelwahab, E.M. Nassef, Treatment of petrochemical wastewater containing phenolic compounds by electrocoagulation using a fixed bed electrochemical reactor, *Int. J. Electrochem. Sci.*, 8 (2013) 1534–1550.
- [13] Directive 2013/39/EU of the European Parliament and of the Council of 12 August 2013 Amending Directives 2000/60/EC and 2008/105/EC as Regards Priority Substances in the Field of Water Policy.
- [14] S. Ghosh, O. Falyouna, A. Malloum, A. Othmani, C. Bornman, H. Bedair, H. Onyeaka, Z.T. Al-Sharif, A.O. Jacob, T. Miri, C. Osagie, S. Ahmadi, A general review on the use of advance oxidation and adsorption processes for the removal of furfural from industrial effluents, *Microporous Mesoporous Mater.*, 331 (2022) 111638, doi: 10.1016/j.micromeso.2021.111638.
- [15] T.A. Saleh, Protocols for synthesis of nanomaterials, polymers, and green materials as adsorbents for water treatment technologies, *Environ. Technol. Innovation*, 24 (2021) 101821, doi: 10.1016/j.eti.2021.101821.
- [16] H. Soni, P. Padmaja, Palm shell based activated carbon for removal of bisphenol A: an equilibrium, kinetic and thermodynamic study, *J. Porous Mater.*, 21 (2014) 275–284.
- [17] M. Zbair, K. Ainassaari, Z. El Assal, S. Ojala, N. El Ouahedy, R.L. Keiski, M. Bensitel, R. Brahmi, Steam activation of waste biomass: highly microporous carbon, optimization of bisphenol A, and diuron adsorption by response surface methodology, *Environ. Sci. Pollut. Res.*, 25 (2018) 35657–35671.
- [18] M.H. Al-Malack, M. Dauda, Competitive adsorption of cadmium and phenol on activated carbon produced from municipal sludge, *J. Environ. Chem. Eng.*, 5 (2017) 2718–2729.
- [19] T.A. Saleh, A.M. Elsharif, S. Asiri, A.-R.I. Mohammed, H. Dafalla, Synthesis of carbon nanotubes grafted with copolymer of acrylic acid and acrylamide for phenol removal, *Environ. Nanotechnol. Monit. Manage.*, 14 (2020) 100302, doi: 10.1016/j.enmm.2020.100302.
- [20] W. Wang, Q. Gong, Z. Chen, W.D. Wang, Q. Huang, S. Song, J. Chen, X. Wang, Adsorption and competition investigation of phenolic compounds on the solid-liquid interface of three-dimensional foam-like graphene oxide, *Chem. Eng. J.*, 378 (2019) 122085, doi: 10.1016/j.cej.2019.122085.
- [21] P. Sudhakar, I.D. Mall, V.C. Srivastava, Adsorptive removal of bisphenol A by rice husk ash and granular activated carbon—a comparative study, *Desal. Water Treat.*, 57 (2016) 12375–12384.
- [22] J. Li, N. Liang, X. Jin, D. Zhou, H. Li, M. Wu, B. Pan, The role of ash content on bisphenol A sorption to biochars derived from different agricultural wastes, *Chemosphere*, 171 (2017) 66–73.
- [23] K. Yang, W. Wu, Q. Jing, L. Zhu, Aqueous adsorption of aniline, phenol, and their substitutes by multi-walled carbon nanotubes, *Environ. Sci. Technol.*, 42 (2008) 7931–7936.
- [24] D. Lin, B. Xing, Adsorption of phenolic compounds by carbon nanotubes: role of aromaticity and substitution of hydroxyl groups, *Environ. Sci. Technol.*, 42 (2008) 7254–7259.
- [25] A. Marszałek, G. Kamińska, N.F. Abdel Salam, Simultaneous adsorption of organic and inorganic micropollutants from rainwater by bentonite and bentonite-carbon nanotubes composites, *J. Water Process Eng.*, 46 (2022) 102550, doi: 10.1016/j.jwpe.2021.102550.
- [26] H. Zhang, M. Xia, F. Wang, P. Li, M. Shi, Adsorption properties and mechanism of montmorillonite modified by two Gemini surfactants with different chain lengths for three benzotriazole emerging contaminants: experimental and theoretical study, *Appl. Clay Sci.*, 207 (2021). <https://doi.org/10.1016/j.clay.2021.106086>.
- [27] S. Kango, S. Kalia, A. Celli, J. Njuguna, Y. Habibi, R. Kumar, Surface modification of inorganic nanoparticles for development of organic-inorganic nanocomposites - A review, *Prog. Polym. Sci.* 38 (2013) 106086, doi: 10.1016/j.clay.2021.106086.
- [28] J. Bohdziewicz, M. Dudziak, G. Kamińska, E. Kudlek, Chromatographic determination and toxicological potential evaluation of selected micropollutants in aquatic environment—analytical problems, *Desal. Water Treat.*, 57 (2016) 1361–1369.
- [29] K. Vasanth Kumar, S. Sivanesan, Sorption isotherm for safranin onto rice husk: comparison of linear and non-linear methods, *Dyes Pigm.*, 72 (2007) 130–133.
- [30] M.Y. Lee, I. Ahmed, K. Yu, C.-S. Lee, K.-K. Kang, M.-S. Jang, W.-S. Ahn, Aqueous adsorption of bisphenol A over a porphyrinic porous organic polymer, *Chemosphere*, 265 (2021) 129161, doi: 10.1016/j.chemosphere.2020.129161.
- [31] K. Vijayalakshmi, B. Mahalakshmi Devi, S. Latha, T. Gomathi, P.N. Sudha, J. Venkatesan, S. Anil, Batch adsorption and desorption studies on the removal of lead(II) from aqueous solution using nanochitosan/sodium alginate/microcrystalline cellulose beads, *Int. J. Biol. Macromol.*, 104 (2017) 1483–1494.